Functional Beta Cell Mass from Device-Encapsulated hESC-Derived Pancreatic Endoderm Achieving Metabolic Control

Thomas Robert,[1,3] Ines De Mesmaeker,[1,3] Geert M. Stangé,[1,3] Krista G. Suenens,[1,3] Zhidong Ling,[1,3] Evert J. Kroon,[2,3] and Daniel G. Pipeleers[1,3,*]

[1]Diabetes Research Center, Brussels Free University-VUB and University Hospital Brussels-UZB, Brussels 1090, Belgium
[2]ViaCyte, Inc., San Diego, CA 92121, USA
[3]BetaCellTherapy Consortium (supported by EU and JDRF), Brussels, Belgium
*Correspondence: daniel.pipeleers@vub.ac.be
https://doi.org/10.1016/j.stemcr.2018.01.040

SUMMARY

Human stem cells represent a potential source for implants that replace the depleted functional beta cell mass (FBM) in diabetes patients. Human embryonic stem cell-derived pancreatic endoderm (hES-PE) can generate implants with glucose-responsive beta cells capable of reducing hyperglycemia in mice. This study with device-encapsulated hES-PE (4×10^6 cells/mouse) determines the biologic characteristics at which implants establish metabolic control during a 50-week follow-up. A metabolically adequate FBM was achieved by (1) formation of a sufficient beta cell number ($>0.3 \times 10^6$/mouse) at >50% endocrine purity and (2) their maturation to a functional state comparable with human pancreatic beta cells, as judged by their secretory responses during perifusion, their content in typical secretory vesicles, and their nuclear NKX6.1-PDX1-MAFA co-expression. Assessment of FBM in implants and its correlation with *in vivo* metabolic markers will guide clinical translation of stem cell-derived grafts in diabetes.

INTRODUCTION

Human stem cells can be efficiently differentiated to pancreatic endoderm (D'Amour et al., 2005, 2006) that forms beta cells following implantation in immune-deficient mice (Kroon et al., 2008; Rezania et al., 2012) or following further *in vitro* steps (Pagliuca et al., 2014; Rezania et al., 2014; Russ et al., 2015). The function of stem cell-generated beta cells was evaluated by measuring their glucose responsiveness, and by assessing their ability to reverse or prevent a diabetic state. This analysis was also conducted in recipients of macro- and micro-encapsulated grafts (Bruin et al., 2013; Motté et al., 2014; Vegas et al., 2016), in which it could be extended to retrieved implants that can be examined *ex vivo* after different post-transplantation periods (Motté et al., 2014). The secretory responses by *in-vitro-* and *in-vivo*-generated beta cells have been compared with those of human pancreatic islet cell isolates with the aim of evaluating their physiological relevance (D'Amour et al., 2006; Motté et al., 2014; Pagliuca et al., 2014; Rezania et al., 2014; Russ et al., 2015). Variability in preparations, conditions, and quality control standards, however, limit this judgment. Little information is available on the composition and biology of stem cell-generated beta cell implants, which represent the basis for achieving the metabolically adequate functions that determine their therapeutic significance. There are also no data on the efficacy of beta cell formation in stem cell-derived preparations and implants, and on its relative abundance with respect to other cell types. Direct analysis of retrieved implants allows combined measurements of number and functional state of beta cells, the two components of the functional beta cell mass (FBM), which represents the key therapeutic target in beta cell replacement (Pipeleers et al., 2008). In this study, we assessed the FBM in device-encapsulated stem cell-derived implants 1 year after their subcutaneous placement, and demonstrated the significance of its components for achieving metabolic control.

In previous work we examined the functional state of beta cells generated over 20 weeks in implants of human embryonic stem cell-derived pancreatic endoderm (hES-PE) (Motté et al., 2014). Freshly prepared hES-PE cells had been loaded in a Theracyte device and implanted subcutaneously in non-obese diabetic (NOD)/severe combined immunodeficiency (SCID) mice. At post-transplant (PT) week 20, implants presented single hormone-positive alpha and beta cells that exhibited rapid secretory responses to increasing and decreasing glucose concentrations, similar to human pancreatic islet cell isolates. However, their insulin secretory amplitude was markedly lower, as also was their cellular insulin content and insulin biosynthetic activity. These characteristics could reflect an immature state of newly formed beta cells, as observed in rodents (Hellerström and Swenne, 1991; Jermendy et al., 2011; Martens et al., 2014). To examine this hypothesis, we analyzed the cells over a 1-year study including markers of differentiation. To evaluate the significance of findings in terms of beta cell replacement we simultaneously determined the number of formed beta cells and examined whether these FBM components were correlated with *in vivo* markers of function and metabolic control.

PT Week	Number of Animals According to Levels (ng/mL) at 15 Min Post-glucose Load				
	<0.5	0.5–1	1–3	3–6	>6
10	7/17	5/17	5/17	0/17	0/17
20	0/19	5/19	7/19	2/19	5/19
50	0/13	0/13	1/13	5/13	7/13

Grafts of hES-PE cells were prepared from three different batches (A, B, and C) and implanted in, respectively 7, 7, and 6 NSG recipients. Technical reasons interfered with plasma C-peptide measurement for three (PT week 10) and one (PT week 20) animals. Three animals were killed at PT week 20 (plasma hu-C-peptide 1–3 ng/mL) for histological analysis of implants, and four died before the endpoint of the study. For virtually all 13 animals that survived until PT week 50, cellular composition (n = 13) and insulin content (n = 12) were determined (Table 2). For eight of them, implants were also analyzed for insulin secretory responses in perifusion (Figure 2; Table 3) and corresponding cell numbers (Table 2); three of these eight with full analysis belonged to the subgroup of five with hu-C-peptide >6 ng/mL at PT week 20, of which one died at PT week 48; the other five belonged to the subgroup that did not reach these levels at that time.

RESULTS

In Vivo Evidence for Increasing FBM in Device-Encapsulated hES-PE Implants over 50 Weeks

A plasma human (hu)-C-peptide level >0.5 ng/mL at 15 min following an intraperitoneal glucose injection was used as an *in vivo* marker for the appearance of hormone-releasing beta cells in hES-PE implants. In none of the recipients was this the case at or before PT week 5. The 0.5 ng/mL level was present in 10/17 NSG mice at PT week 10 and in all at PT week 20 (Table 1). Levels between PT weeks 20 and 50 were followed to detect recipients with a loss or increase in FBM over this period: all exhibited progressively increasing concentrations, however in a wide range (0.6–7.9 ng/mL at PT week 20, 1.8–23.7 ng/mL at PT week 50), which is indicative for individual differences in further FBM development. When analyzed as a group, plasma hu-C-peptide values increased 9-fold between PT weeks 10 and 30, after which the further increase was only 26%, leveling off between PT weeks 40 and 50 (Figure 1A).

Over the first 20 weeks, the increase was similar to that in NOD/SCID mice, the strain followed in parallel as a control reference to our previous study over this period. At PT week 15, both strains reached levels that were measured in recipients of human pancreatic islet cell grafts with 10^6 beta cells (40×10^6/kg body weight [BW]) transplanted in the kidney capsule (1.2 ± 0.3 ng/mL), and then increased with time beyond these levels while those in islet cell implants decreased (Figure 1A).

In both NSG and NOD/SCID recipients of hES-PE implants, the increase in plasma hu-C-peptide levels was preceded by a 2-fold increase in fasting plasma glucagon levels, starting between PT weeks 3 and 7, and persisting until PT week 50 in NSG mice (Figure 1A), as previously reported.

Ex Vivo Determination of Beta Cell Number in Implants at PT Week 50

Combined stainings of insulin, glucagon and somatostatin antibodies indicated the absence of polyhormonal cells (Figure S1), and could thus be used to determine the respective percentages in the implants, and, consequently, the respective cell numbers when combined with total nuclear counts (Table 2).

At PT week 50, cell number varied between 13% and 97% of the number inserted in the devices. Beta cell numbers ranged from 15 to 600×10^3 per implant, a variability that correlated with the observed variability in plasma hu-C-peptide levels at that time (Figure 1B) and earlier. We indeed noticed that mice with plasma hu-C-peptide >6 ng/mL from PT week 20 onward presented markedly higher beta cell numbers at PT week 50 than the others (Table 2); they were therefore further considered as a subgroup with high FBM and investigated for its functional characteristics.

Linear regression analysis not only showed that plasma hu-C-peptide levels at PT week 50 were positively correlated to the number of beta cells but also to the number of alpha cells (Figure 1B), as well as to the endocrine purity of the implants (data not shown). The subgroup with high FBM exhibited >50% endocrine cell purity versus 20% in that with low FBM (Table 2). This degree of purity was similar to that in cultured human pancreatic islet cell preparations as used in clinical transplantation (Table 2). Remarkably, both subgroups presented a higher percentage of glucagon-positive than insulin-positive cells, which contrasts with their relative proportion in pancreatic islet cell isolates (Table 2).

Ex Vivo Analysis of Functional State of Beta Cells in Implants at PT Week 50

At PT week 50, the functional state of retrieved beta cells was analyzed by measuring their secretory responsiveness to glucose and the size of their hormone storage, and by identifying their expression of differentiation markers. Data were compared with those of beta cells in cultured human pancreatic islet cell preparations as used in clinical transplantation.

hES-PE-generated beta cells exhibited a higher basal release rate (at 2.5 mmol/L glucose) than human pancreatic beta cells, but the difference was not statistically significant (Figure 2; Table 3). Increases to 5, 10, or 20 mmol/L glucose
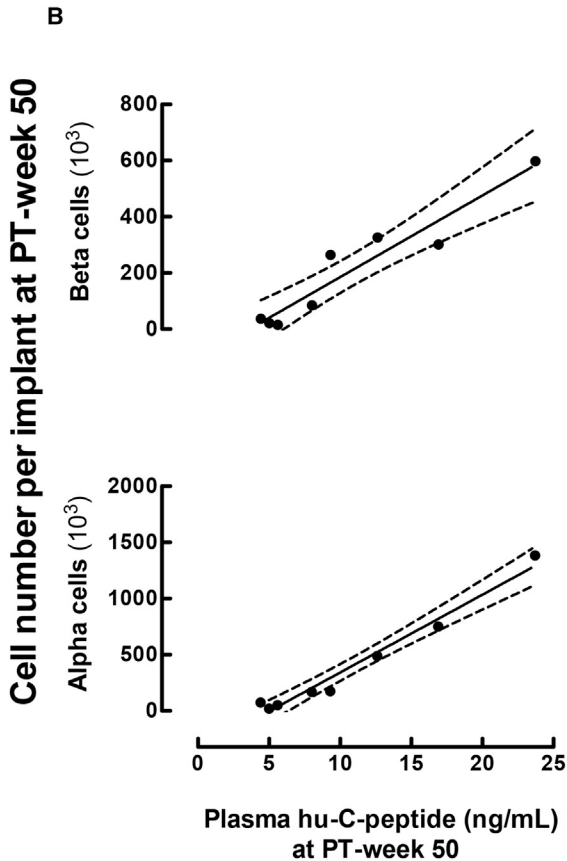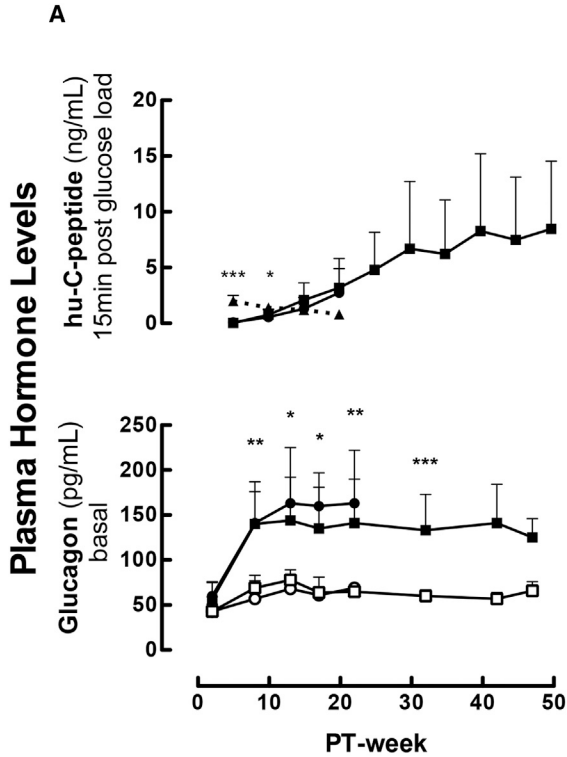
A

B

Figure 1. Development of FBM in Device-Encapsulated hES-PE Implants Followed over 50 Weeks

(A) Plasma hu-C-peptide (15 min after intraperitoneal glucose load) and glucagon levels (basal, 2 hr fast) (means ± SD) in NSG-recipient mice (filled squares, n = 20) increased during the first 20 weeks as in NOD/SCID recipients (filled circles, n = 19), the strain also used in our previous study (Motté et al., 2014). NOD/SCID control mice (n = 9) are plotted as empty circles. Plasma hu-C-peptide became consistently detectable from PT week 10 onward, and increased in all animals to levels stabilizing between weeks 30 and 50.

Plasma hu-C-peptide levels are also shown for NOD/SCID recipients of human pancreatic islet cells (10^6 beta cells/recipient) under the kidney capsule (triangles, dotted line); they were significantly higher than values in hES-PE recipients at PT weeks 5 and 10 (***$p < 0.0001$ and *$p < 0.05$ by one-way ANOVA with Tukey's *post-hoc* test, respectively), but became lower at later time points.

Plasma glucagon in NSG recipients was higher than in controls (empty squares, n = 7) from PT weeks 7 to 32 (*$p < 0.05$; **$p < 0.01$; ***$p < 0.001$ by one-way ANOVA with Tukey's *post-hoc* test); after which the difference was no longer statistically significant.

(B) At PT week 50, plasma hu-C-peptide levels correlated with the number of beta cells and the number of alpha cells in the retrieved implants (linear regression with 95% confidence interval of, respectively, $r_p = 0.9555$; $R^2 = 0.9130$; $p = 0.0002$, and $r_p = 0.9857$; $R^2 = 0.9716$; $p < 0.0001$).

induced an equally rapid rise in released insulin, reaching similar amplitudes whether expressed in absolute terms (pg insulin/10^3 beta cells/min) or as a percentage of cellular insulin content (Figure 2; Table 3). Both preparations maintained a second phase release during prolonged exposure to 20 mmol/L glucose, and equally rapidly suppressed release following a switch to 2.5 mmol/L glucose-basal medium (Figure 2). The amplitude of first phase response to 10 mmol/L glucose was higher than that to 5 mmol/L, but not further increased at 20 mmol/L. This higher release rate was not maintained during the second phase unless glucagon was added (Table 3). We did not observe differences in secretory responsiveness and amplitudes between the subgroups with high and low FBM when expressing data per number of perifused beta cells (data not shown); there was also no difference in their respective cellular insulin content (Table 2). The higher glucose-induced plasma hu-C-peptide levels that were measured in the subgroup with high FBM from PT week 20 onward can thus not be attributed to a higher glucose responsiveness or higher insulin store of the formed beta cells, i.e., their functional state.

Stem cell-generated beta cells contained a smaller insulin reserve than cultured pancreatic beta cells isolated from donor organs (11.2 ± 3.6 versus 16.8 ± 2.7 ng/10^3 beta cells, $p < 0.05$ by Student's t test). They were single-hormone positive, as was also the case at PT week 20, contrasting with the polyhormonal cells at start (Figure S1).

Table 2. Endocrine Cell Composition in hES-PE Implants at PT Week 50

	Cellular Composition (% of Total Population)				Beta Cell Number		Insulin Content	
	(n)	INS	GCG	SST	(n)	10^3 per Implant	(n)	ng/10^3 Beta Cells
hES-PE implants at PT week 50								
All analyzed implants	(13)	7 ± 6***	14 ± 11	7 ± 2	(8)	205 ± 206	(11)	11.2 ± 3.6
Subgroups based on PT week 20 plasma hu-C-peptide:								
0.5–6 ng/mL	(10)	5 ± 3***	9 ± 6	6 ± 2	(5)	85 ± 104	(8)	11.2 ± 4.2
>6 ng/mL	(3)	15 ± 3***	31 ± 5* °°	10 ± 0* °	(3)	408 ± 165	(3)	11.2 ± 2.4
Cultured human pancreatic islet cell aggregates	(9)	35 ± 9	14 ± 3	5 ± 1		NA	(4)	16.8 ± 2.7

Comparison with cultured human pancreatic islet cells. Data express means ± SD for representative samples from implants retrieved at PT week 50 after gentle dispersion with collagenase. Values from cultured human pancreatic islet cell isolates serve as a reference. INS, insulin; GCG, glucagon; SST, somatostatin. Number of implants analyzed for each assay (n) is indicated in columns. Statistical differences by one-way ANOVA with Tukey's *post-hoc* test: hES-PE implants versus human islet cells: *$p < 0.05$; ***$p < 0.001$. hES-PE implants from high C-peptide (>6 ng/mL) subgroup versus low C-peptide (0.5–6 ng/mL) subgroup: °$p < 0.05$; °°$p < 0.01$.

At PT weeks 20 and 50, they exhibited typical beta cell secretory vesicles (Figure S1), with a wide halo around granules with varying form and electron density, which markedly differs from the dense granules without halo in the start preparation. Pale granules, considered to contain higher proportions of proinsulin, were present in comparable percentages (17% ± 11% and 16% ± 9% at PT weeks 20 and 50), similar to those in cultured human pancreatic beta cells (15% ± 9%); this is consistent with the similar proinsulin over C-peptide molar ratios measured by immunoassays in the respective cellular extracts (all under 5%; data not shown).

Stem cell-generated beta cells in the implants expressed nuclear transcription factors that are characteristic for adult human beta cells, i.e., PDX1, NKX6.1, and MAFA (Figure 3). The start preparation did not contain MAFA-positive nuclei, and its cells with PDX1- and NKX6.1-positive nuclei were not insulin positive. Nuclear co-staining for PDX1, NKX6.1, and MAFA occurred in increasing percentages over time (25% ± 8% and 53% ± 21% at, respectively, PT weeks 20 and 50), approaching the values in adult human pancreas (71% ± 18%) (Figure 3). The latter value is the mean of measurements in five donor organs (ranging from 40% to 83% per pancreas), using automated segmentation analysis software. It is consistent with previous work showing that not all insulin-positive cells in human adult islet tissue are MAFA positive (Guo et al., 2013). Its higher percent positivity (71% versus 58% in Guo et al.) may be related to use of intact human pancreatic tissue instead of isolated islets, to variability in donor organs, to differences in quantification method, and/or MAFA antibody used. Virtually no nuclear MAFA staining was detected in insulin-negative cells.

Metabolic Effect of Human Stem Cell-Derived Implants with High FBM

The subgroup with high FBM, as marked by plasma hu-C-peptide >6 ng/mL from PT week 20 onward, exhibited a lower glycemia at basal (2 hr fasting) and at 15 min post-glucose load than age-matched controls (Figure 4) or the subgroup with low FBM (data not shown). This was associated with a suppression of plasma mouse C-peptide levels measured under these conditions at all time points (Figure 4), as well as with a lower pancreatic total insulin content (20 ± 8 versus 44 ± 5 μg in controls, p < 0.01 by Student's t test) at PT week 50; their pancreas glucagon content was also lower (29 ± 7 versus 43 ± 21 ng in controls), but not statistically so. The suppression of mouse beta cells during glucose stimulation indicates that the human beta cell secretory response of the implants determined the return of hyperglycemia to basal levels within 75 min (glycemia at 90 and 120 min post-glucose load was not statistically different from levels at the start). It would have been interesting to measure human and mouse C-peptide and glucagon levels over 120 min following a glucose load, but this was technically not possible in the present experiment.

Identification of Non-endocrine Cells in Implants at PT Week 50

At PT weeks 20 and 50, virtually all non-endocrine cells corresponded to vimentin- or cytokeratin (CK)-positive cells (Figure S2); no amylase-positive cells were found. CK cells formed ductal structures and were also positive for CK19, indicating their pancreatic phenotype (Figure S2). The non-endocrine cells, as labeled by vimentin or CK, were responsible for the majority of KI67-positive cells that were found scattered over the sections (Figure S3). The
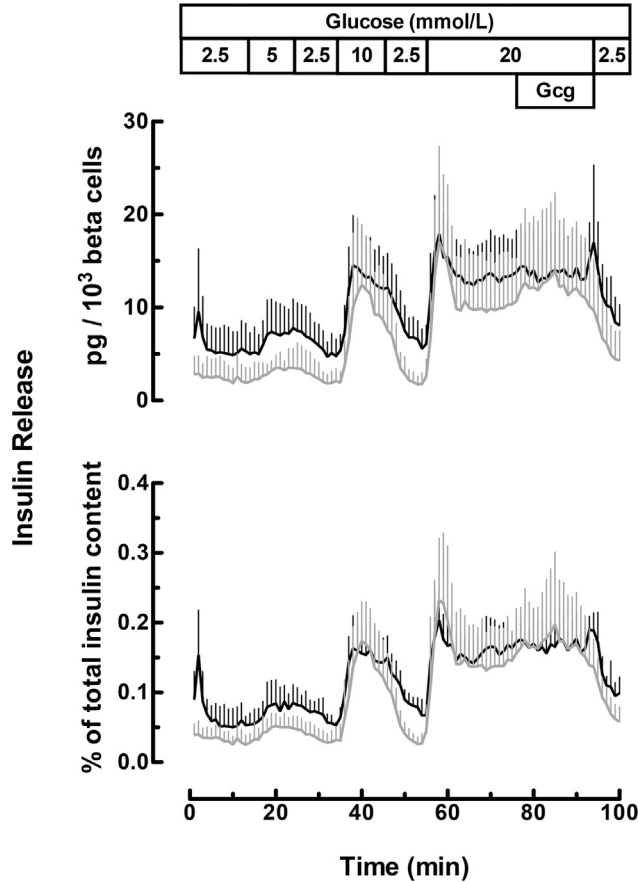
Figure 2. Glucose Responsiveness of Insulin Release by hES-PE Implants Retrieved at PT Week 50

Data express means ± SD of insulin release by hES-PE implants retrieved at PT week 50 (black curve, n = 8) and by cultured human pancreatic islet cell isolates (gray curve, n = 7). Both preparations were perifused at varying glucose concentrations. The response to 20 mmol/L glucose was first measured in the absence and then in the presence of glucagon (10^{-8} mol/L). Insulin was measured in the perifusate fractions and expressed per 10^3 beta cells (top) or as percent of cellular insulin content (bottom).

percentage of KI67-positive cells was low (0.7%–1.5% of all cells in the sections), tending to be lower than at start or at PT week 20 (1.7%–3.4%). While these data are not indicative for the existence of an actively proliferating cell population, other study designs are needed to investigate the significance of cell replication in the development and biology of these hES-PE-generated implants.

For none of the three hES-PE batches used in this study did we observe teratoma formation in the implants. For one of them, ciliated CK-positive cells were noticed, lining larger ducts with a cylindric epithelium that also contained goblet-like cells (Figure S4); these CK cells were also positive for CK7, a marker reported in transition epithelia as well as in pancreatic ducts (Bouwens et al., 1994). Electron micro-

scopy confirmed the presence of ciliae at the luminal side of ducts (Figure S4).

DISCUSSION

This study shows that device-encapsulated implants of hES-PE can generate, within 1 year, an FBM that achieves and maintains metabolic control in immune-compromised mice. It defines requirements for this FBM at the level of its two components: the number of beta cells and their functional state. It compares the composition and function of metabolically adequate implants with those in human pancreatic islet cell preparations that were shown to exert metabolic effects following intraportal transplantation in type 1 diabetes patients (Keymeulen et al., 2006).

The hES-PE source used was previously shown to differentiate to beta cells following transplantation as a free graft in the kidney capsule, fat pad, or subcutis (Kroon et al., 2008; Motté et al., 2014), or encapsulated in a TheraCyte device (Motté et al., 2014). Cryopreserved batches were now used to fill Encaptra devices (ViaCyte, San Diego, CA) with 4×10^6 cells before subcutaneous implantation in normoglycemic NSG mice, exposing their *in vivo* differentiation to higher glucose levels than in normal humans (average basal 130 ± 15 versus 70–100 mg/dL). Generation of hormone-releasing beta cells was monitored through appearance and levels of plasma hu-C-peptide after acutely increasing glycemia above 400 mg/dL. At PT week 20 all recipients presented circulating hu-C-peptide, but levels varied considerably (0.6–7.9 ng/mL) as well as the time at which they had first appeared: those with >6 ng/mL (>2 nmol/L) were already hu-C-peptide positive at PT week 10; this further increased to levels that were maintained throughout PT week 50, while decreasing basal glycemia to the human range (mean 84 ± 8 versus 135 ± 4 mg/dL in control mice). The associated suppression of mouse C-peptide release and decline in mouse pancreatic insulin content indicated that the stem cell-generated beta cells in these implants exerted glucose control. This suppression and lowering of basal glycemia was not observed in recipients with lower hu-C-peptide levels.

In this study, we opted to examine the formation of an FBM in normoglycemic mice. Subsequent work can then investigate the effects of a hyperglycemic state upon this process. It should, however, be noted that alloxan-induced diabetes, with its sustained glycemia of >400 mg/dL, does not mimic the diabetic state in patients who exhibit markedly lower average levels under insulin treatment. In fact, the presently used normoglycemic mice create a mildly hyperglycemic state for human beta cells in their implant. Under the selected conditions, more than 20 weeks were needed to establish implants with a functionally mature

Table 3. Comparison of Glucose-Induced Insulin Release by hES-PE Implants with that by Cultured Human Pancreatic Islet Cells

|	hES-PE Implant PT Week 50 (n=8)	Cultured Human Pancreatic Islet Cells (n=7)
Insulin release (pg/10^3 beta cells/min)		
Basal (2.5 mmol/L glucose)	5.2 ± 1.8	2.0 ± 1.2
Glucose-induced first-phase release		
5 mmol/L glucose	7.9 ± 3.3	3.6 ± 1.0
10 mmol/L glucose	14.8 ± 4.7***, °	12.8 ± 7.0*
20 mmol/L glucose	17.2 ± 4.7***, °°°	17.1 ± 8.0***, °°
Glucose-induced second-phase release		
20 mmol/L glucose	12.6 ± 3.6	9.3 ± 5.1
20 mmol/L glucose +10 nmol/L glucagon	14.7 ± 4.2[†]	13.8 ± 8.5[†]
Insulin release (% of insulin content)		
Basal (2.5 mmol/L glucose)	0.06 ± 0.02	0.03 ± 0.02
Glucose-induced first-phase release		
5 mmol/L	0.09 ± 0.03	0.05 ± 0.02
10 mmol/L	0.17 ± 0.04***, °°	0.18 ± 0.06***, °°°
20 mmol/L	0.20 ± 0.03***, °°°	0.25 ± 0.08***, °°°

Data (means ± SD) represent average of three consecutive fractions with highest values during first 5 min following medium change to higher glucose concentration (first-phase) or following glucagon addition (second-phase), and of the three last fractions at 20 mmol/L glucose before glucagon addition (second-phase). Statistical differences within each preparation by one-way ANOVA with Tukey's *post hoc* test: first-phase release versus basal: *p < 0.05; ***p < 0.001; first-phase release at 10 and 20 mmol/L glucose versus 5 mmol/L: °p < 0.05; °°p < 0.01; °°°p < 0.001; second-phase release at 20 mmol/L with or without glucagon versus first-phase release at 5 mmol/L: [†]p < 0.05; second-phase release at 20 mmol/L with or without glucagon versus first-phase release at 10 mmol/L: no significant difference.

beta cell mass of sufficient size to exert metabolic control. Our data indicate that the characteristics of human beta cell implants that correct this "hyperglycemic" state in the period between PT weeks 20 and 50, decreasing glycemia to the level for which human beta cells, are programmed. They also demonstrate the usefulness of normoglycemic mice to assess glycemic control by human beta cell implants. Further studies should assess whether these implants can also maintain metabolic control during and following episodes of frankly elevated glycemia, as can occur in diabetes patients. The presently reported implant analysis can then be implemented to examine whether the identified key components of this potential come under threat.

The ability to quantitatively retrieve implants from the devices allowed to identify the FBM characteristics that achieve metabolic control. This involved the formation of a sufficient number of beta cells, on average 0.4×10^6 per implant (16×10^6 beta cells/kg BW), and their maturation toward a functional state that was similar to that of cultured human pancreatic beta cell preparations used in our clinical transplant program, where they are intraportally injected at a dose of $2–6 \times 10^6$ beta cells/kg BW (Gillard et al., 2013; Keymeulen et al., 2006). These preparations exert metabolic effects in C-peptide-negative type 1 diabetes recipients and can thus be considered as a relevant reference in the present *in vivo* and *ex vivo* studies. When implanted under the kidney capsule at 10^6 beta cells/mouse (40×10^6/kg BW), plasma hu-C-peptide levels reached 2 ng/mL until PT week 8, but then declined, which contrasts with the high (>6 ng/mL) and sustained (up to PT week 50) levels achieved by stem cell-generated beta cell implants containing markedly less beta cells.

Despite loading of the same cell number per device (4×10^6), we observed a marked variability in time of appearance of hu-C-peptide in plasma, as well as its levels, during the 50-week follow-up period. This was reflected in a variability in cellular composition of the implants at PT week 50, both in terms of cell number (recovery of 13%–97% of initial number) and percentages of endocrine cells (10%–63% within recovered cells), which parallel each other, i.e., higher endocrine purity when higher cell recovery. This outcome could result from differences in the degree of cell survival during tissue integration of the devices
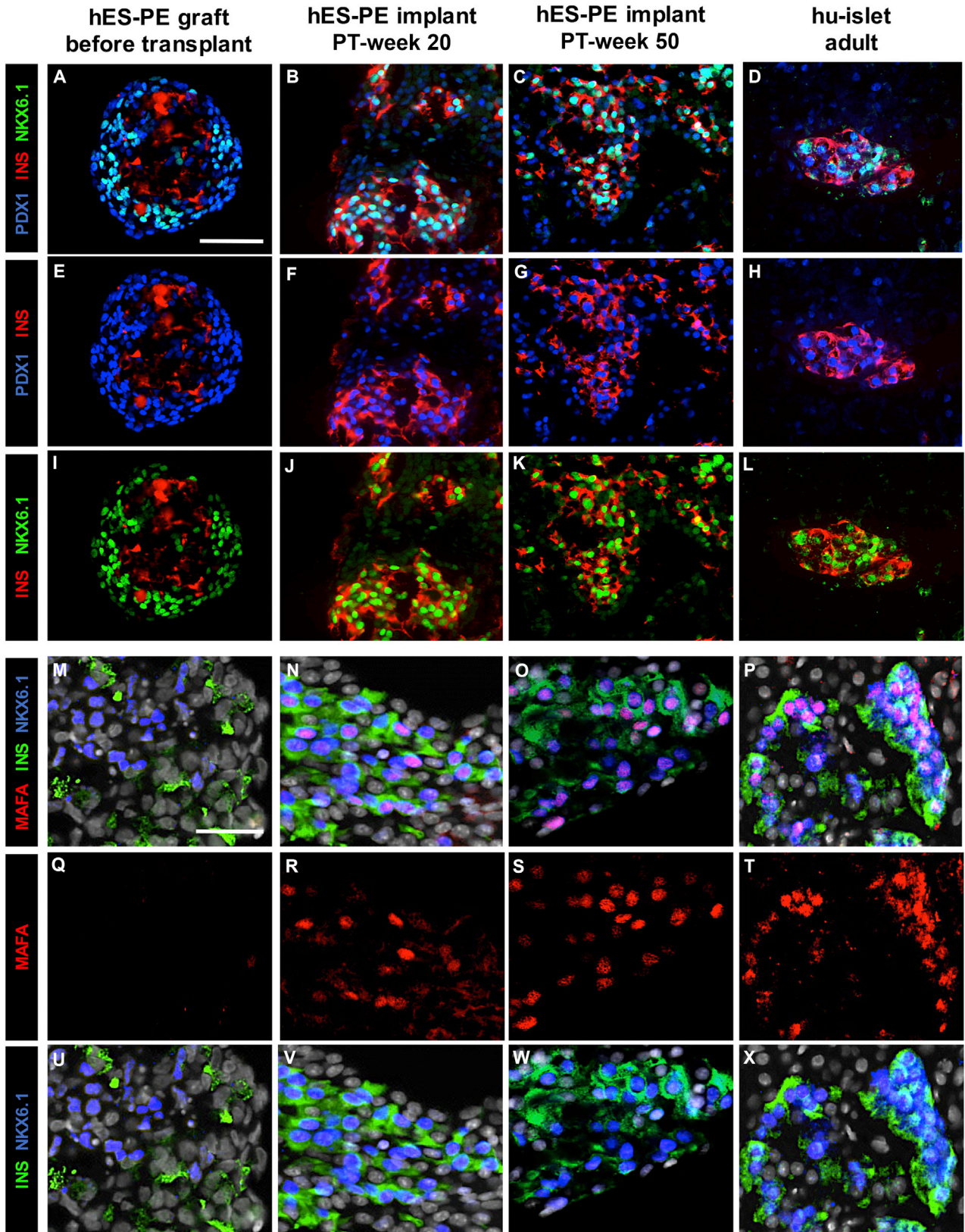
(legend on next page)

and associated influences on the degree of endocrine differentiation. We could not statistically assign a batch-related influence; the three hES-PE preparations exhibited similar cell composition and high viability (>90%) at the start, while each resulted in implants with variable outcome. The presently reported variability in implant composition and related *in vivo* outcome may also occur in other laboratories examining effects of stem cell-generated beta cell implants. Identifying its reasons should help improve standardization and the outcome of this type of implant, and indicate factors that increase the degree of their endocrine differentiation. Since tissue healing and vascularization around implants are considered as important variables, (pre)treatment of the implant sites could positively direct their influence (Pepper et al., 2015). In a recent study with non-encapsulated hES-PE implants in the subcutis, correction of hyperglycemia was only achieved following a vascularizing pretreatment (Pepper et al., 2017). *Ex vivo* analysis of implants retrieved at different times post-transplantation can indicate to which extent such pretreatment increases and or maintains cell survival, endocrine differentiation, and/or beta cell maturation.

During our 50-week study in non-diabetic NSG mice, all device-encapsulated hES-PE implants differentiated to an FBM with sustained and biologically relevant plasma hu-C-peptide levels (all glucose-responsive with 12/13 exceeding 3 ng/mL). Plasma hu-C-peptide appeared between PT weeks 5 and 10, and then progressively increased up to PT week 40 and, for some animals, beyond that time. Use of *in-vitro*-generated beta cells (stage 6 or stage 7 cells in stem cell differentiation) instead of their PE-precursor stage (stage 4) can be expected to lead to its earlier detection. This was indeed the case in the study of Rezania et al. (2014) using another hES source and transplanting free grafts under the kidney capsule; however, hu-C-peptide levels in stage 6 or 7 recipients also markedly increased during a 20-week follow-up (up to >3 ng/mL), indicating further *in vivo* development of an FBM; this development was also associated with a decrease in glycemia, as well as with considerable variability (Rezania et al., 2014). There are, so far, no data on outcome of stage 6 or 7 cells in a subcutaneous device, nor on its correlation with characteristics of the implants. The function of stage 7 cells has been demonstrated within alginate-microcapsules that

had been injected in the peritoneal cavity of diabetic immune-competent mice (Vegas et al., 2016); they maintained plasma hu-C-peptide levels over 20 weeks while correcting hyperglycemia; these levels were, however, much lower (around 0.6 ng/mL in average), which can explain why glycemia did not decrease to the human range (Vegas et al., 2016).

The presence of glucose-induced C-peptide release, as seen for stem cell-derived implants at PT week 20, is not sufficient to conclude that functionally mature beta cells have been formed. Rapidity, dose dependency, and amplitude of glucose secretory responses can serve as markers, in particular when compared with those of quality-controlled human pancreatic beta cell preparations. Perifusion of hES-PE-generated beta cells retrieved at PT week 20 showed rapid responsiveness to increasing or decreasing glucose concentrations, as is to be expected from physiologically operating beta cells (Motté et al., 2014). The amplitude of glucose-induced insulin release was lower than that for pancreatic human beta cell aggregates, but this difference was no longer observed at PT week 50, as shown in the present study. In both preparations, first-phase release rates were now comparable being dose-dependently stimulated by glucose with a maximum at 10 mmol/L glucose; addition of glucagon maintained these rates during the second phase at 20 mmol/L. Although cultured human pancreatic beta cell isolates might well functionally differ from beta cells in their natural habitat, and thus present limitations as physiologic reference, these findings strongly suggest that hES-PE implants require more than 20 weeks to generate functionally (more) mature beta cells. Evidence for this time-dependent maturation comes also from the percentages of insulin-positive cells with nuclear expression of MAFA, the transcription factor with the primary role in adult beta cell activity (Hang et al., 2014). While, at PT week 20, all insulin-positive cells were positive for NKX6.1 and PDX1, and negative for glucagon and somatostatin, only 25% exhibited a nuclear MAFA positivity. This fraction increased to 53% at PT week 50, still lower than in the adult human pancreas (71% ± 18%), but this is not statistically significant, and thus possibly indicates that the stem cell-derived beta cell population has not yet matured to the stage of the majority of adult human pancreatic beta cells; their lower cellular insulin content is compatible with

Figure 3. Expression of Beta Cell-Specific Transcription Factors in Insulin-Positive Cells of hES-PE Implants
(A–L) The hES-PE aggregates in the graft exhibited peripherally located INS-negative cells with nuclear co-expression of NKX6.1 and PDX1, whereas centrally located INS-positive cells were negative for these transcription factors (A, E, and I). At PT weeks 20 and 50 virtually all INS-positive cells presented nuclear positivity for PDX1 (B, C, F, and G) and NKX6.1 (B, C, J, and K), as in human pancreatic beta cells (D, H, and L). Scale bar, 50 μm.
(M–X) Nuclear expression of MAFA was absent in hES-PE at the start (M, Q, and U), but clearly present at PT weeks 20 and 50 and restricted to insulin-positive cells. The percentage of MAFA + INS + cells increased from 25% ± 8% at PT week 20 (N, R, and V) to 53% ± 21% at PT week 50 (p < 0.01) (O, S, and W), approaching that in the adult human pancreas (P, T, and X) (71% ± 18%). Scale bar, 25 μm.
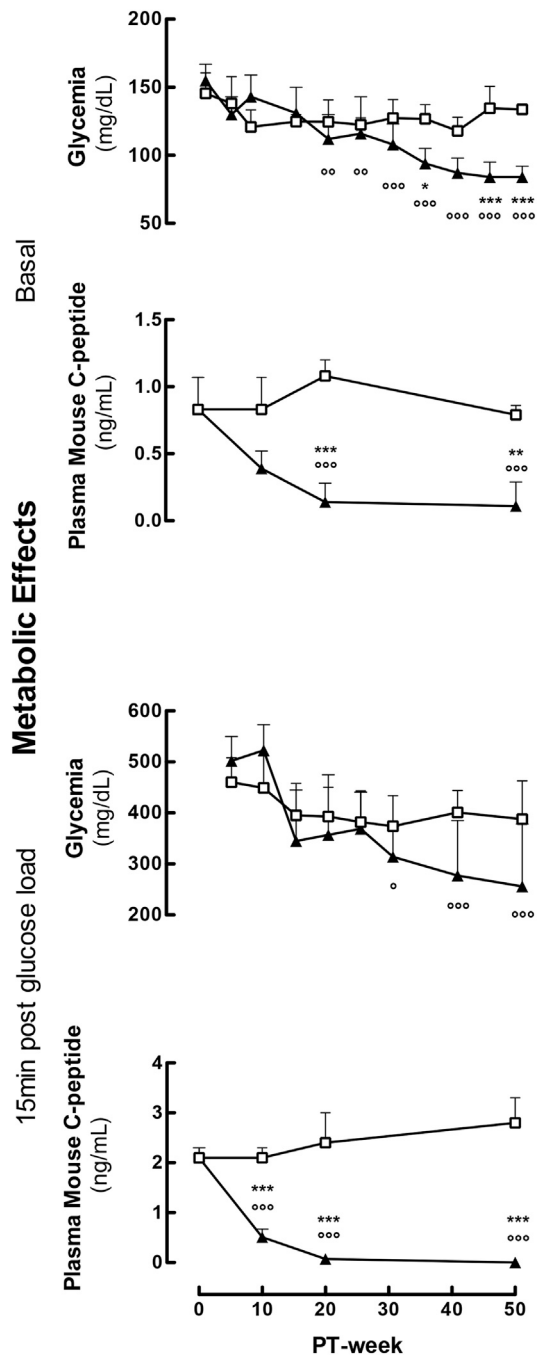
Figure 4. Metabolic Effects in Subgroup of Recipients with hu-C-Peptide Levels >6 ng/mL from PT Weeks 20 to 50

Basal glycemia and plasma mouse C-peptide levels decreased under levels measured at PT week 0 ($^{\circ\circ}p < 0.01$; $^{\circ\circ\circ}p < 0.001$) and in controls (empty squares, n = 4–7, $^*p < 0.05$; $^{**}p < 0.01$; $^{***}p < 0.001$). Both parameters were also lower following intra-peritoneal glucose load (statistical difference with PT week 5: $^{\circ}p < 0.05$; $^{\circ\circ\circ}p < 0.001$, and with controls: $^{***}p < 0.001$). Values are expressed as means ± SD.

this possibility. Electron micrographs showed the presence of the characteristic beta cell secretory vesicles at both PT weeks 20 and 50, with similar proportions of pale lower density granules as in adult pancreatic beta cells, which is in line with the measurement of similar proinsulin over C-peptide ratios in plasma, a marker for a normal proinsulin conversion rate in the cells.

At PT week 50, the glucose-induced plasma hu-C-peptide levels correlated with the number of beta cells in the implant. It can thus be hypothesized that this was also the case at earlier time points, suggesting that the subgroup with levels >6 ng/mL at PT week 20 had formed more beta cells, but still required further maturation to amplify the cellular secretory response. A correlation was also found with the number of alpha cells, which might reflect more favorable conditions for endocrine cell formation and survival in these implants. The higher endocrine purity of implants with the higher FBM is consistent with this view. It is presently unknown whether these alpha cells exerted influences on the development and activities of the FBM in the implants; we recently reviewed evidence supporting their role in pancreatic islet cell implants (Pipeleers et al., 2016). At variance with pancreatic islet cell preparations, the proportion of alpha cells in hES-PE implants at PT week 50 was consistently higher than that of beta cells. While implants with the highest function exhibited a similar endocrine purity as pancreatic islet cell isolates (average of 56% versus 54%), their alpha cell fraction was 2-fold higher, being 2-fold more abundant than beta cells. A higher proportion of alpha cells was also observed by other groups in non-encapsulated hES-PE implants (Pepper et al., 2017; Rezania et al., 2012), suggesting that the device is not responsible for preferential formation and/or survival of alpha cells. In contrast with the mixed endocrine cell composition of implants generated by hES-PE (stage 4), implants of beta cell-containing stage 6 or 7 cells present low or negligible proportions of alpha cells (Pagliuca et al., 2014; Rezania et al., 2014), a difference that should be considered in interpreting and comparing outcome. Such a comparative study could also indicate, be it indirectly, whether the early increase in plasma glucagon levels, as observed for our hES-PE implants, is related to the presence, or early differentiation of glucagon-containing cells.

The non-endocrine cell types present in macro-encapsulated hES-PE implants at PT week 50 are similar as to those identified at earlier stages (Bruin et al., 2013; Motté et al., 2014). Their proportion is variable (37%–90%), which primarily results from the variability in endocrine cell formation and survival. The number of non-endocrine cells per implant was indeed in a more narrow range (0.4–1.7×10^6 cells per implant) than that of endocrine cells (0.08–2.4×10^6 cells per implant). They were

predominantly composed of CK19-positive cells forming ducts and vimentin-positive cells dispersed in the interstitium, without apparent signs of interference with the formation of endocrine cell aggregates. A small proportion of them is KI67 positive, together representing the majority of the 0.7%–1.5% KI67 cells in the implants; this percentage is not higher than that observed in younger human pancreases (Köhler et al., 2011). Comparison with data reported for human pancreatic tissue should, however, take into account their underestimation as a result of postmortem reduction in KI67 staining (Sullivan et al., 2015). A separate study using another experimental design is needed to examine the process of cell proliferation in hES-PE-generated implants. With a recovery of 13%–97% of the implanted cells, the present data are not directly indicative for an expansion of cells within 50 weeks.

In summary, macro-encapsulated hES-PE implants can generate, within 1 year, an FBM that achieves and maintains potent glucose responsiveness and metabolic control in mice. This involves formation of a sufficient number of beta cells and maturation of their functional state toward that of adult human pancreatic beta cells. Other islet endocrine cells, i.e., alpha and delta cells, are also formed, together 2-fold more than beta cells, raising the possibility of their paracrine and/or endocrine role. Our study demonstrates the usefulness of *ex vivo* quantitative analysis of implant composition and function to follow the achievement of FBM properties that appear to be needed to establish *in vivo* markers of metabolic success. This approach should also help to identify interfering factors and causes for variability within and between laboratories. Its implementation is expected to guide translation to beta cell replacement in type 1 diabetes patients, a clinical phase that has been initiated with the device and hES-PE cells that were investigated in the present laboratory study (Schulz, 2014) (ClinicalTrials.gov identifier NCT02239354).

EXPERIMENTAL PROCEDURES

In Vivo Follow-Up of Mice with Device-Encapsulated hES-PE Implants

ViaCyte shipped three batches of cryopreserved hES-PE to Brussels; they were prepared from the CyT49 cell line (Schulz et al., 2012). After thawing, aggregates were cultured for 72 hr in db-N50-K50-E50 (D'Amour et al., 2006; Schulz et al., 2012) before loading 4×10^6 cells per Encaptra device. The Encaptra drug delivery system has been engineered by ViaCyte (EN20, www.viacyte.com) and reported earlier (Agulnick et al., 2015). It is a variant of the Theracyte device, the principle and elements of which have been reviewed (Emerich and Orive, 2017). Encaptra passed a battery of biocompatibility testing per ISO 10993 leading to its use in a clinical phase 1 study (ClinicalTrials.gov identifier NCT02239354). Devices were im-

planted subcutaneously in NOD.Cg-PrkdcscidIl2rgtm1Wjl/SzJ mice (NSG) and NOD.CB17-Prkdc^scid/J mice (NOD/SCID) (Charles River, France). NSG mice were selected for the present long-term study instead of the previously used NOD/SCID mice (Motté et al., 2014) that are prone to thymoma development upon aging; we included NOD/SCID recipients for a 20-week follow-up in order to detect possible differences in *in vivo* outcome versus NSG recipients, as well as versus our previous observations. The term "graft" is used for cell preparations before transplantation and "implant" for tissue that has been implanted. Procedures were approved by the Ethical Committee of Vrije Universiteit Brussel (VUB), and carried out according to the European Community Council Directive (86/609/ EEC). Mice were followed up to 50 weeks with plasma taken at basal (2 hr food removal) and 15 min after intraperitoneal glucose injection (3 g/kg BW). Plasma proinsulin and human (hu-)C-peptide were measured by trefoil-type time-resolved fluorescence immunoassay (De Pauw et al., 2008), plasma glucagon by a commercial kit (Merck Millipore, MA), and blood glucose using Glucocard (Menarini Diagnostics, Italy).

Explantation of hES-PE Implants for *In Situ* and *Ex Vivo* Analysis

At PT weeks 20 and 50, devices were retrieved and hES-PE implants removed for analysis. For *in situ* histology, tissue with inner membrane was fixed in formaldehyde. For *ex vivo* analysis, it was gently dispersed to aggregates <500 μm, using collagenase (type XI, 1 mg/mL, Sigma-Aldrich, MO) supplemented, when necessary, with DNase (2 μg/mL, Roche, Switzerland) and trypsin (5 μg/mL, Sigma-Aldrich). Samples were taken for viability assay and nuclear count (NucleoCounter YC-100, ChemoMetec, Denmark), for immunocytochemistry, for insulin release and cellular insulin assays.

Samples of 250 to 500×10^3 cells were perifused on a Bio-Gel column (P2 Fine, Bio-Rad Laboratories, Hercules, CA) (Motté et al., 2014). After a 60-min wash at 2.5 mmol/L glucose, cells were exposed to 10-min pulses of 5, 10, or 20 mmol/L glucose, with or without 10 nmol/L glucagon, alternating with 10-min returns to basal medium. One-minute perifusate fractions were assayed for insulin and data expressed per number of beta cells and per cellular insulin content.

Cellular hormone content was determined in aggregates before and after perifusion, and before transplantation. Samples were extracted in acetic acid and dried before insulin (Motté et al., 2014) and glucagon (Mercodia, Sweden) assays. Data were expressed per beta or alpha cell number as counted in parallel samples. The hormones were also assayed in the pancreatic organs of mouse recipients following snap freezing in liquid nitrogen and storage at −80°C.

Cellular composition of retrieved implants was evaluated by immunocytochemistry, and compared with that in grafts. Samples were fixed in formaldehyde before embedding in paraffin (*in situ* histology) or araldite (immunocytochemistry on grafts and dispersed aggregates retrieved from implants). Sections underwent heat-induced antigen retrieval (2100-Retriever; PickCell Laboratories, the Netherlands) in citrate (ScyTek Laboratories, UT), EDTA (Klinipat, the Netherlands), or protease (Sigma-Aldrich) buffer. Immunocytochemical stainings were performed with guinea pig anti-insulin and rabbit anti-somatostatin (each 1/1,000, in house produced), mouse anti-glucagon (1/500; g2654; Sigma-Aldrich),

goat anti-PDX1 (1/100, af2419; R&D Systems, MN), mouse anti-NKX6.1 (1/100, monoclonal antibody developed by Ole Madsen, Hagedorn Research Institute, was obtained from the Developmental Studies Hybridoma Bank, created by the NICHD of the NIH, and maintained at The University of Iowa, Department of Biology, Iowa City, IA 52242), rabbit anti-MAFA (1/1,000, a kind gift of Dr Rezania when at BetaLogics, Janssen R&D, NJ) (Rezania et al., 2013), rabbit anti-vimentin (1/100, ab92547; Dako, Denmark), mouse anti-chromogranin A (1/300, MU126-UC; Biogenex, CA), rabbit anti-cytokeratin (1/200, Z0622; Dako), mouse anti-CK19 (1/20, M0888; Dako), and anti-Ki67 (1/100, DRM004; Acris, Germany). Secondary antibodies were Alexa Fluor-conjugated F(ab')$_2$ fragments of affinity-purified antibodies allowing multiple labeling (1/500, Jackson Laboratories, PA), biotinylated anti-mouse secondary antibody followed by an avidin-biotin peroxidase reaction for CK7. Nuclei were stained by DAPI (Sigma-Aldrich) added to mounting medium (Dako). Digital images were acquired on an Axioplan 2 (Carl Zeiss, Germany) microscope with an Orca-R2 camera (Hamamatsu Photonics, Japan) and analyzed with SmartCapture 3 software (DSUK, UK). For automated segmentation analysis of nuclear transcription factor expression, large images from different sections were acquired with a BD Pathway 435 microscope and analyzed in Attovision v1.6 (BD Biosciences, CA). Data were processed using FlowJo v10.1 (FlowJo, OR).

For electron microscopy, samples were fixed in glutaraldehyde (2.5% in sodium cacodylate), post-fixed in 1% osmium-tetroxide, stained in 2% uranyl acetate, dehydrated in ethanol, immersed in propylene oxide, and embedded in Poly/bed 812 Araldite resin (Polysciences, Germany). Ultrathin sections (50–100 nm) were mounted on copper grid, treated with lead citrate, and examined in a Tecnai-10 electron microscope (Philips, the Netherlands). Digital images were taken with a MegaViewG2 CCD camera (EMSIS, Germany), and granule numbers and cytoplasmic area measured with ImageJ open-source platform.

Human Pancreatic Tissue and Islet Cell Isolates

Human pancreatic tissue sections were provided by the Diabetes Biobank, and cultured human pancreatic islet cell isolates (n = 7; 3–50 days culture, average 17 ± 14 days) by the Beta Cell Bank, both at VUB-affiliated University Hospital Brussels. Isolation and culture methods have been previously described (Ling and Pipeleers, 1996); functional, compositional, and structural analysis occurred as outlined for hES-PE grafts and implants. These materials were used according to the guidelines of the Eurotransplant Foundation, with approval by the institutional ethical committee.

Statistical Analysis

Results are expressed as means ± SD. Statistical analysis was performed using Prism 5.0 (GraphPad, CA) for comparison by one-way ANOVA with Tukey's *post-hoc* test or Student's t test (statistical significance at $p < 0.05$).

SUPPLEMENTAL INFORMATION

Supplemental Information includes four figures and can be found with this article online at https://doi.org/10.1016/j.stemcr.2018.01.040.

REFERENCES

Agulnick, A.D., Ambruzs, D.M., Moorman, M.A., Bhoumik, A., Cesario, R.M., Payne, J.K., Kelly, J.R., Haakmeester, C., Srijemac, R., Wilson, A.Z., et al. (2015). Insulin-producing endocrine cells differentiated in vitro from human embryonic stem cells function in macroencapsulation devices in vivo. Stem Cells Transl. Med. *4*, 1214–1222.

Bouwens, L., Wang, R.N., De Blay, E., Pipeleers, D.G., and Kloppel, G. (1994). Cytokeratins as markers of ductal cell differentiation and islet neogenesis in the neonatal rat pancreas. Diabetes *43*, 1279–1283.

Bruin, J.E., Rezania, A., Xu, J., Narayan, K., Fox, J.K., O'Neil, J.J., and Kieffer, T.J. (2013). Maturation and function of human embryonic stem cell-derived pancreatic progenitors in macroencapsulation devices following transplant into mice. Diabetologia *56*, 1987–1998.

D'Amour, K.A., Agulnick, A.D., Eliazer, S., Kelly, O.G., Kroon, E., and Baetge, E.E. (2005). Efficient differentiation of human embryonic stem cells to definitive endoderm. Nat. Biotechnol. *23*, 1534–1541.

D'Amour, K.A., Bang, A.G., Eliazer, S., Kelly, O.G., Agulnick, A.D., Smart, N.G., Moorman, M.A., Kroon, E., Carpenter, M.K., and Baetge, E.E. (2006). Production of pancreatic hormone-expressing endocrine cells from human embryonic stem cells. Nat. Biotechnol. *24*, 1392–1401.

Emerich, D., and Orive, G. (2017). Cell Therapy, Current Status and Future Directions (Springer).

Gillard, P., Hilbrands, R., Van de Velde, U., Ling, Z., Lee, D.H., Weets, I., Gorus, F., De Block, C., Kaufman, L., Mathieu, C., et al. (2013). Minimal functional beta cell mass in intraportal implants that reduces glycemic variability in type 1 diabetic recipients. Diabetes Care *36*, 3483–3488.

Guo, S., Dai, C., Guo, M., Taylor, B., Harmon, J., Sander, M., Robertson, R.P., Powers, A., and Stein, R. (2013). Inactivation of specific β cell transcription factors in type 2 diabetes. J. Clin. Invest. *123*, 3305–3316.

Hang, Y., Yamamoto, T., Benninger, R.K.P., Brissova, M., Guo, M., Bush, W., Piston, D.W., Powers, A.C., Magnuson, M., Thurmond, D.C., et al. (2014). The MafA transcription factor becomes essential to islet ß-cells soon after birth. Diabetes *63*, 1994–2005.

Hellerström, C., and Swenne, I. (1991). Functional maturation and proliferation of foetal pancreatic b-cells. Diabetes *40*, 89–93.

Jermendy, A., Toschi, E., Aye, T., Koh, A., Aguayo-Mazzucato, C., Sharma, A., Weir, G.C., Sgroi, D., and Bonner-Weir, S. (2011). Rat neonatal beta cells lack the specialised metabolic phenotype of mature beta cells. Diabetologia *54*, 594–604.

Keymeulen, B., Gillard, P., Mathieu, C., Movahedi, B., Maleux, G., Delvaux, G., Ysebaert, D., Roep, B., Vandemeulebroucke, E., Marichal, M., et al. (2006). Correlation between beta cell mass and glycemic control in type 1 diabetic recipients of islet cell graft. Proc. Natl. Acad. Sci. USA *103*, 17444–17449.

Köhler, C.U., Olewinski, M., Tannapfel, A., Schmidt, W.E., Fritsch, H., and Meier, J.J. (2011). Cell cycle control of beta cell replication in the prenatal and postnatal human pancreas. Am. J. Physiol. Endocrinol. Metab. *300*, E221–E230.

Kroon, E., Martinson, L.A., Kadoya, K., Bang, A.G., Kelly, O.G., Eliazer, S., Young, H., Richardson, M., Smart, N.G., Cunningham, J., et al. (2008). Pancreatic endoderm derived from human embryonic stem cells generates glucose-responsive insulin-secreting cells in vivo. Nat. Biotechnol. *26*, 443–452.

Ling, Z., and Pipeleers, D.G. (1996). Prolonged exposure of human beta cells to elevated glucose levels results in sustained cellular activation leading to a loss of glucose regulation. J. Clin. Invest. *98*, 2805–2812.

Martens, G.A., Motté, E., Kramer, G., Stangé, G., Gaarn, L.W., Hellemans, K., Nielsen, J.H., Aerts, J.M., Ling, Z., and Pipeleers, D. (2014). Functional characteristics of neonatal rat β cells with distinct markers. J. Mol. Endocrinol. *52*, 11–28.

Motté, E., Szepessy, E., Suenens, K., Stangé, G., Bomans, M., Jacobs-Tulleneers-Thevissen, D., Ling, Z., Kroon, E., and Pipeleers, D. (2014). Composition and function of macroencapsulated human embryonic stem cell-derived implants: comparison with clinical human islet cell grafts. Am. J. Physiol. Endocrinol. Metab. *307*, E838–E846.

Pagliuca, F.W., Millman, J.R., Gürtler, M., Segel, M., Van Dervort, A., Ryu, J.H., Peterson, Q.P., Greiner, D., and Melton, D.A. (2014). Generation of functional human pancreatic β cells in vitro. Cell *159*, 428–439.

De Pauw, P.E., Vermeulen, I., Ubani, O.C., Truyen, I., Vekens, E.M., van Genderen, F.T., De Grijse, J.W., Pipeleers, D.G., Van Schraven-

dijk, C., and Gorus, F.K. (2008). Simultaneous measurement of plasma concentrations of proinsulin and C-peptide and their ratio with a trefoil-type time-resolved fluorescence immunoassay. Clin. Chem. *54*, 1990–1998.

Pepper, A.R., Gala-Lopez, B., Pawlick, R., Merani, S., Kin, T., and Shapiro, A.M. (2015). A prevascularized subcutaneous device-less site for islet and cellular transplantation. Nat. Biotechnol. *33*, 518–523.

Pepper, A.R., Pawlick, R., Bruni, A., Wink, J., Rafiei, Y., O'Gorman, D., Yan-Do, R., Gala-Lopez, B., Kin, T., MacDonald, P., et al. (2017). Transplantation of human pancreatic endoderm cells reverses diabetes post transplantation in a prevascularized subcutaneous site. Stem Cell Reports *8*, 1689–1700.

Pipeleers, D., Chintinne, M., Denys, B., Martens, G., Keymeulen, B., and Gorus, F. (2008). Restoring a functional beta-cell mass in diabetes. Diabetes Obes. Metab. *10*, 54–62.

Pipeleers, D., Robert, T., De Mesmaeker, I., and Ling, Z. (2016). Concise review: markers for assessing human stem cell-derived implants as β-cell replacement in type 1 diabetes. Stem Cells Transl. Med. *5*, 1338–1344.

Rezania, A., Bruin, J.E., Riedel, M.J., Mojibian, M., Asadi, A., Xu, J., Gauvin, R., Narayan, K., Karanu, F., O'Neil, J.J., et al. (2012). Maturation of human embryonic stem cell-derived pancreatic progenitors into functional islets capable of treating pre-existing diabetes in mice. Diabetes *61*, 2016–2029.

Rezania, A., Bruin, J.E., Xu, J., Narayan, K., Fox, J.K., O'Neil, J.J., and Kieffer, T.J. (2013). Enrichment of human embryonic stem cell-derived NKX6.1-expressing pancreatic progenitor cells accelerates the maturation of insulin-secreting cells in vivo. Stem Cells *31*, 2432–2442.

Rezania, A., Bruin, J.E., Arora, P., Rubin, A., Batushansky, I., Asadi, A., O'Dwyer, S., Quiskamp, N., Mojibian, M., Albrecht, T., et al. (2014). Reversal of diabetes with insulin-producing cells derived in vitro from human pluripotent stem cells. Nat. Biotechnol. *32*, 1121–1133.

Russ, H.A., Parent, A.V., Ringler, J.J., Hennings, T.G., Nair, G.G., Shveygert, M., Guo, T., Puri, S., Haataja, L., Cirulli, V., et al. (2015). Controlled induction of human pancreatic progenitors produces functional beta-like cells in vitro. EMBO J. *34*, 1759–1772.

Schulz, T.C. (2014). Concise review: manufacturing of pancreatic endoderm cells for clinical trials in type 1 diabetes. Stem Cells Transl. Med. *4*, 927–931.

Schulz, T.C., Young, H.Y., Agulnick, A.D., Babin, M.J., Baetge, E.E., Bang, A.G., Bhoumik, A., Cepa, I., Cesario, R.M., Haakmeester, C., et al. (2012). A scalable system for production of functional pancreatic progenitors from human embryonic stem cells. PLoS One *7*, e37004.

Sullivan, B.A., Hollister-Lock, J., Bonner-Weir, S., and Weir, G.C. (2015). Reduced Ki67 staining in the postmortem state calls into question past conclusions about the lack of turnover of adult human beta cells. Diabetes *64*, 1698–1702.

Vegas, A.J., Veiseh, O., Gürtler, M., Millman, J.R., Pagliuca, F.W., Bader, A.R., Doloff, J.C., Li, J., Chen, M., Olejnik, K., et al. (2016). Long-term glycemic control using polymer-encapsulated human stem cell–derived beta cells in immune-competent mice. Nat. Med. *22*, 306–311.